Environmental Science
Water Research & Technology

Reduction of Scaling in Microwave Induced Membrane Distillation on Carbon Nanotube Immobilized Membrane

Journal:	*Environmental Science: Water Research & Technology*
Manuscript ID	EW-ART-02-2019-000153.R1
Article Type:	Paper
Date Submitted by the Author:	28-Mar-2019
Complete List of Authors:	Humoud , Madihah Saud ; New Jersey Institute of Technology Intrchom, Worawit; New Jersey Institute of Technology Roy, Sagar; New Jersey Institute of Technology, Chemistry & Environmental Science Mitra, Somenath; New Jersey Institute of Technology

Water Impact:

The thermal as well as the non-thermal effects of microwave induced (MI) irradiation was utilized as a means to heat and reduce the fouling of the highly concentrated salt solutions via membrane distillation (MD). The MIMD process exhibited enhanced desalination performances in terms of pure water generation and less fouling compared to the conventional system.

Reduction of Scaling in Microwave Induced Membrane Distillation on Carbon Nanotube Immobilized Membrane

Madihah Saud Humoud, Worawit Intrchom, Sagar Roy and Somenath Mitra*

Department of Chemistry and Environmental Science,

New Jersey Institute of Technology

Newark, NJ, 07102

USA

* Corresponding Author

Somenath Mitra, 973-596-5611(t), 973-596-3586(F), somenath.mitra@njit.edu

Abstract

Membrane distillation (MD) is an emerging technology that has much potential in desalination and the treatment of saline waste. Although MD has shown its ability to treat high saline waters, membrane fouling is still one of the major issues that limits the long-term stability performances of MD. In this paper, we report the reduction in scaling during microwave induced membrane distillation (MIMD), where the feed water is heated by microwave irradiation instead of conventional thermal heaters. MD was carried out using a carbon nanotube immobilized membrane using highly concentrated aqueous calcium carbonate, calcium sulfate and barium sulfate solutions, and it was observed that the decline in flux over time was significantly less in MIMD. As compared to conventional heating, the salt deposition on the membrane was 50-79 % less during microwave heating. Scanning Electron microscopy analysis also showed that morphologies of the deposited salts from MIMD were different from those from conventional MD. The decrease in scale formation was also confirmed by dynamic light scattering studies which showed that microwave heating formed smaller particles than via conventional heating. The study clearly demonstrated that MIMD not only generated higher flux, but also had significantly less fouling with the inorganic scalants studied here.

Keywords: Desalination; scaling; microwave; membrane distillation; water vapor flux

1. Introduction

With water scarcity looming all over the horizon, the generation of potable water from sea/brackish water as well as the saline waste management are becoming important desalination technologies. Desalting is also important for zero to minimal liquid discharge (ZLD) systems that eliminate liquid waste from production facilities by recovering all salts and reusing the purified water [1-3]. Typical ZLD units use thermal distillation techniques because Reverse osmosis (RO) has limited applicability at high salinity encountered in ZLD [4, 5].

Compared to conventional thermal distillation, the relatively low temperature operation (50–90°C) and the lower CAPEX (capital expenditure) make membrane distillation (MD) an attractive alternative [6-9]. In MD, the driving force is a temperature induced vapor pressure gradient generated by having a hot feed and a cold permeate [10]. The low operating temperature in MD makes desalination possible using low grade heat sources such as low pressure steam and solar energy [11-17]. Compared to reverse osmosis (RO) a major advantage of MD is that while the former uses dense hydrophilic membranes, MD uses microporous hydrophobic membranes that are less prone to fouling, and MD can be used to treat water with higher salinity [18-21].

To make MD commercially viable, it is important to address some of its limitations such as low water vapor flux, fouling at high salt concentrations and high energy consumption [18, 22-28]. Since MD can be used for treating high salt concentration waters, some major commercial opportunities for MD are the treatment of RO reject, power plant blow downs and produced water from oil and gas production [18, 29-32]. One of the anticipated problems with increased salt concentrations is scaling where flux decreases due to the deposition of suspended or dissolved substances on the membrane [18, 19]. Membrane processes are susceptible to scaling at higher salt concentrations when the ionic product of sparingly

soluble salts in the concentrated feed exceeds its equilibrium solubility product [33]. Some common scalants are calcium salts such as calcium carbonate ($CaCO_3$), Calcium sulfate ($CaSO_4$) and barium sulfate ($BaSO_4$) [18-20]. Numbers of studies have reported different approaches to scaling control [34-36]. The use of ultrasound has been studied as an effective technique to enhance the membrane performance and membrane cleaning [34], the introduction of nano-bubbles in ceramic membrane has shown improved fouling resistance [35] and micro-bubble aeration has been investigated in vacuum MD resulting in the improved desalination performance [36]. All of these process modifications require additional energy that may increase the operational cost as well as carbon foot print. The use of antiscalants is another conventional way to mitigate the fouling [37], however, the presence of antiscalants may hinder the precipitation of salts present in the concentrate [38], which require additional separation steps [39]. The other methods also have some disadvantages, such as, the ultrasound may damage the membrane during long term operation and the control of feed solution pH needs additional chemicals, which may affect the membrane stability and need further separation steps. On the other hand, the MIMD does not affect the membrane and is a clean process that does not require additional chemicals.

Microwave heating has generated some interest in the membrane community recently. The microwave induced photo-catalysis has been couple to membrane processes[40-42] and microwave induced vacuum membrane distillation has been reported[43]. Recently, we have reported microwave induced membrane distillation (MIMD) for desalination where the feed water is heated by microwave instead of conventional thermal heaters [44]. The mechanism of microwave heating is quite different from conventional heating [44, 45]. In general, saline water generates dipoles when placed in a microwave field which then develops orientation polarization, and the lag between the dipole orientation and the electric field leads to heating of the water [46-49]. In addition, non-thermal effects such as local super heating and generation

of nanobubbles are associated with microwave heating [43, 50-52]. Together these lead to lower temperature polarization, higher vapor pressure gradient and flux [53]. The microwave process is also known to reduce the activation energy of physical and chemical processes, break down hydrogen bonded structures and reduce the average particle size salts in an aqueous environments [43, 53-56]. The energy consumption in MIMD has also been reported to be significantly lower than that by regular heating [43, 44, 57, 58]. Our previous study has demonstrated enhanced flux compared to regular MD with highly concentrated aqueous sodium chloride (NaCl) solution and showed higher ionic mobility that indicated the possibility of reduced fouling via microwave heating [44]. Based on the results so far, MIMD seems to be a promising technique, where the microwave radiation appeared to break down salt water clusters. Therefore, it was deduced that MIMD may exhibit altered fouling behavior, and it is important to study the scaling in MIMD resulting from common inorganic foulants. This is a goal of the present study.

Particle size of the dissolved solute is one of the key factors that influences membrane fouling. In general, it has been observed that the particles with smaller size tend to lower the fouling tendency [44]. Since important parameters such as hydrogen bonding and surface tension are affected by microwave radiations, the latter also affects the colloidal behavior of salts [44, 59-61]. Both crystal growth and decomposition which refers to the breakdown of salt crystals are effected by microwave radiations [62]. Since the mechanism of salt crystals formation in microwave is known to be quite different [63, 64], therefore, it is expected that the fouling behavior in MIMD will vary from conventional heating. The objective of this research is to explore the effect of microwave heating on fouling in a MD process, especially in the presence of common foulants such as calcium and barium salts.

2. Experimental

2.1. Chemicals, materials and membrane module

$CaSO_4$ (99% pure, anhydrous), $CaCO_3$ (98+%, pure heavy powder), and $BaSO_4$ (99%, precipitated) were obtained from Fisher Scientific (Hanover Park, IL) and deionized water (Barnstead 5023, Dubuque, Iowa) were used in all experiments.

The carboxylated carbon nanotubes (CNT-COOH) were incorporated on the polypropylene (PP) membrane (A carbon nanotube immobilized membrane (CNIM) was used in this study. The base membrane was a polypropylene (PP) membrane (0.45 μm pore size, STERLITECH company, WA, US) to fabricate the carbon nanotube immobilized membrane (CNIM). The details for CNT-COOH synthesis and CNIM fabrication have been reported before [27, 65].

2.2 Experimental setup

The MIMD setup for this experiment is shown in **Figure 1** and it has been described in our previous work [44]. A polytetrafluoroethylene (PTFE) module with an effective membrane area of 11.94 cm^2 has been used for DCMD experiments. The experimental setup includes the membrane module, pumps (Cole Parmer, Vernon Hills, IL) for feed and permeate flow, temperature controlled water bath (GP-200), a circulating chiller (MGW Lauda RM6) and a microwave (Oster, OGZF1301). A temperature controlled water bath was used to heat the feed water for conventional MD and an 1100-watt domestic microwave for MIMD. The experiments were carried out at different feed flow rates and temperatures with constant permeate flow rate of 200 mL/min at 15^oC. K-type temperature probes (Cole Parmer) were used to monitor the temperatures of the system. The permeate water quality was monitored using a conductivity meter (Jenway, 4310). Under similar conditions, each of the experiment was conducted for three times. The relative standard deviation was found less than 1%.

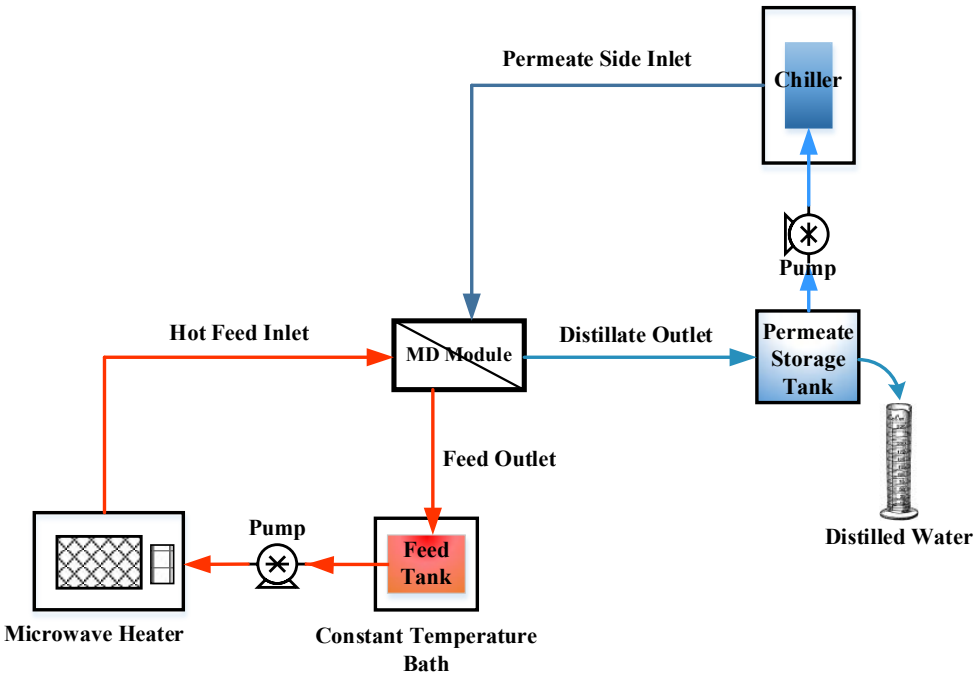

Figure 1. Schematic of microwave induced membrane distillation system.

2.3. Membrane performances

The performance of MIMD, especially its fouling characteristics with CNIM was investigated using $CaSO_4$, $CaCO_3$, and $BaSO_4$ solutions at the concentrations of 2950, 3500 and 2500 ppm respectively. Comparisons were made with conventional MD. The water vapor permeate flux was used to determine the performance of MIMD and MD with varying feed temperatures and flow rates. The water vapor flux, J_w, is expressed as:

$$J_w = \frac{W_p}{t \cdot A} \qquad (1)$$

where, *Wp* is the total mass of permeate, t is the operation time and A is the effective membrane surface area. To compare fouling in conventional MD and MIMD, the flux was measured over a period of time and the normalized flux decline, FD_n, was measured as:

$$FD_n\,(\%) = \left(1 - \frac{J_f}{J_o}\right) x\ 100 \qquad (2)$$

Where, J_f and J_0 are the final permeate flux and initial flux, respectively.

The deposition of salt crystals was characterized by scanning electron microscopy (SEM) (JEOL; model JSM-7900F, JEOL USA inc., USA) and quantified using gravimetric measurements (Perkin Elmer, TGA 8000). Dynamic light scattering (Zetasizer Nano-ZS90, Malvern Instrument Ltd, UK) was used to determine the sizes of salt particles in simulated conventional and microwave heating. The water and salt-water interactions with microwave heating were characterized using Fourier transform infrared spectroscopy (FTIR) (IRAffinity-1, Shimadzu).

3. Results and Discussion

3.1. Effect of temperature and feed flowrate on water vapor flux

Figure 2a shows the effect of temperature on water vapor flux in MD and MIMD. Highly concentrated $CaSO_4$ solution was used as the feed. The permeate fluxes of both MD and MIMD with CNIM increased with increase in temperatures as the water vapor pressure increased with temperature. It was observed that MIMD provided higher permeate flux at all temperatures when compared with the conventional MD. The highest enhancement was found at the feed temperature of 50°C with permeate flux of 38.6 kg/m^2.h, which was 90 % higher than conventional MD. This is in line with our previous work [44].

The effect of varying feed flow rate at 70^{o}C is shown in **Figure 2b.** The permeate flow rate was kept constant at 200 ml/min. Increase in feed flow rates increased the water vapor fluxes of both MIMD and MD. The increased feed flow rate not only increases the amount of water vapor into the MD module, but created a turbulence and decreased the boundary layer effect at the bulk feed solution-membrane interface. As a result, the temperature polarization decreased and the permeate flux was enhanced. In general, these results are in line with our previous study with NaCl [44]**.** The enhancements in MIMD were

attributed to the microwave effects such as localized super heating, nanobubbles formation, breakdown of hydrogen-bonded H_2O and salt-water cluster destruction. However, it is noted that the enhancements reported here for $CaSO_4$ were higher than those reported for NaCl [44]. The scaling tendency of $CaSO_4$ is much higher compared to the NaCl solution. The reduction in particle size and other non-thermal effect of microwave heating significantly lessen the membrane fouling via salt deposition and hence enhanced the desalination performances.

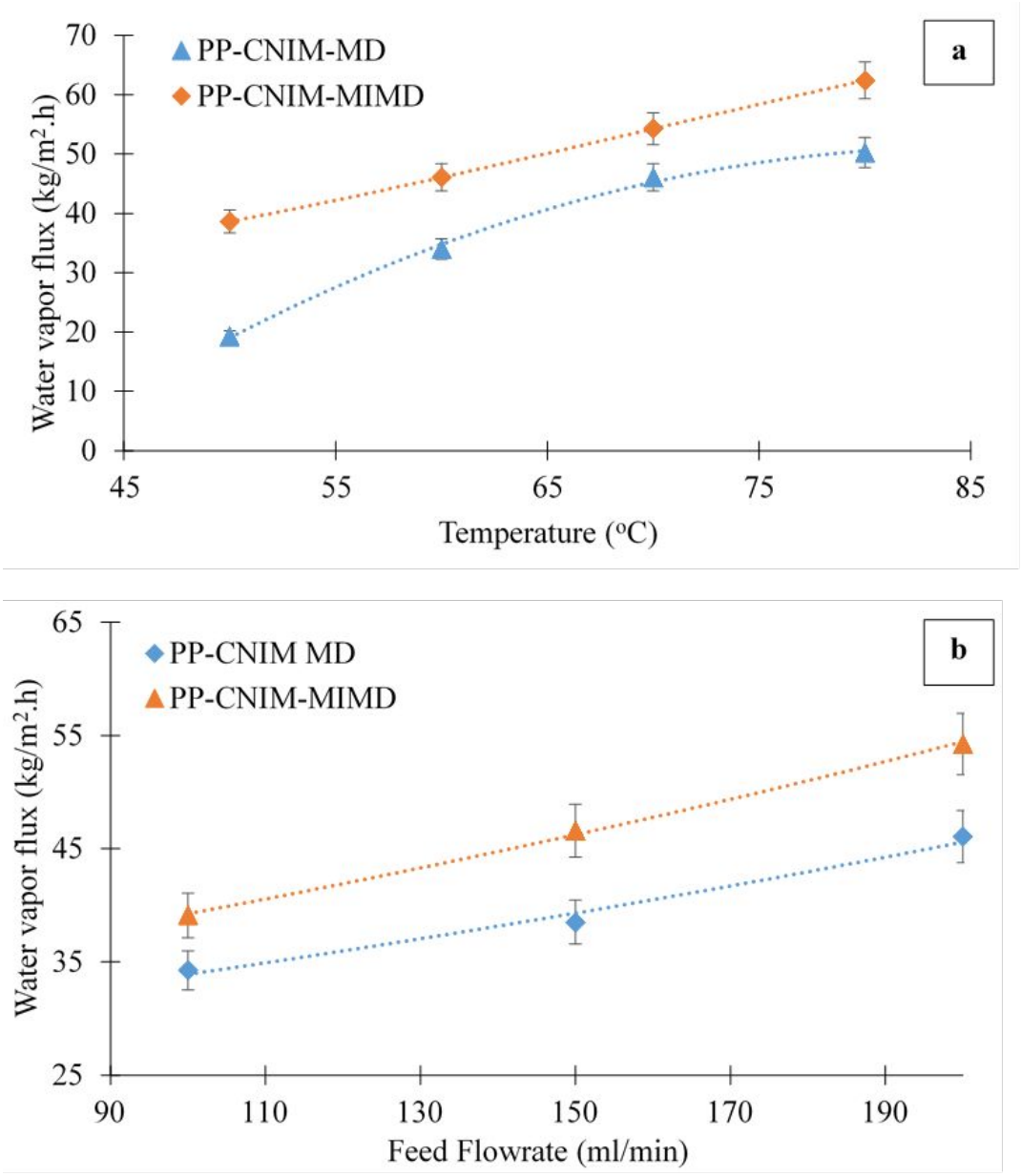

Figure 2. Effect of increasing **a)** feed temperature and **b)** flow rate on water vapor flux for $CaSO_4$ solution during MD and MIMD.

3.2 Membrane fouling in MD and MIMD

As already mentioned, the membrane fouling in MIMD was studied using highly concentrated salt solutions such $CaSO_4$, $CaCO_3$, and $BaSO_4$, and compared to the conventional MD. These concentrations were clearly higher than what is normally encountered and were used only to test the level of fouling. Fouling was investigated by the reduction of flux over the period of operation time. All experiments were carried out at a feed temperature of 70^{o}C and feed flow rate of 200 ml/min. Figure 3a, 3b, and 3c show the water vapor flux as a function of time for $CaSO_4$, $CaCO_3$, and $BaSO_4$, respectively. The reduction in water vapor flux with time showed that fouling was quite serious with the salt solutions tested for both MIMD and MD.

Figure 3a shows that the water vapor flux was 46.1 kg/m^2.h at the first hour for conventional MD with $CaSO_4$ solution, while it was 54.3 kg/m^2.h for MIMD. The flux for MD dropped to 12.6 kg/m^2.h after 12 h of continuous operation. The flux reduction pattern was somewhat different for MIMD, where the flux reduced rapidly within the first four hours and then gradually decreased to 23.5 kg/m^2.h after 12 h, which was 86.5 % higher than that of MD. The initial and final permeate fluxes were used to calculate the normalized flux decline. The results show that the normalized flux decline of MD and MIMD with $CaSO_4$ were 72.7% and 56.7%, respectively.

Figure 3b illustrates the water vapor flux of MIMD and MD with $CaCO_3$. The flux for MD was 50.1 kg/m^2.h, while it was 55.3 kg/m^2.h for MIMD at the first hour. The flux decline was much slower for $CaCO_3$ than $CaSO_4$. The flux of MD modestly dipped and ended up at 32.4 kg/m^2.h after 20 hrs. For MIMD, the water vapor flux had the same trend as $CaSO_4$ with the significant reduction in the first five hours, followed by the gradual decrement and

the flux was 40.2 kg/m^2.h after the operation of 20 h, which was 24.1% higher than that of MD. The normalized flux decline of MD was 35.6%, while the value of MIMD was 27.3%.

Figure 3c shows the fluxes of MD and MIMD for $BaSO_4$ with 16 h of continuous operation. The initial flux was 50.1 kg/m^2.h for MD and gradually decreased to 33.5 kg/m^2.h after 16-h operation. At the same time the flux of MIMD was 54.4 kg/m^2.h at the first hour and gradually reduced to 38.5 kg/m^2.h after 16 h, which is 14.9% higher than that of MD. The normalized flux decline of MD and MIMD with $BaSO_4$ were 33.4% and 29.2%, respectively. The normalized flux decline of the three salts calculated at the operation time of 12 h showed that $CaSO_4$ was the strongest foulant and this was in agreement with results published previously [44]. The results also shown that $BaSO_4$ was the stronger foulant compared to $CaCO_3$. It was also evident that the microwave heating provided not only higher water vapor flux than MD, but also the fouling was less compared to conventional heating. The fouling intensities of CaSO4, CaCO3 and BaSO4 salts were observed to be different that may be due to the difference in solubility, deposition and crystal formation rate.

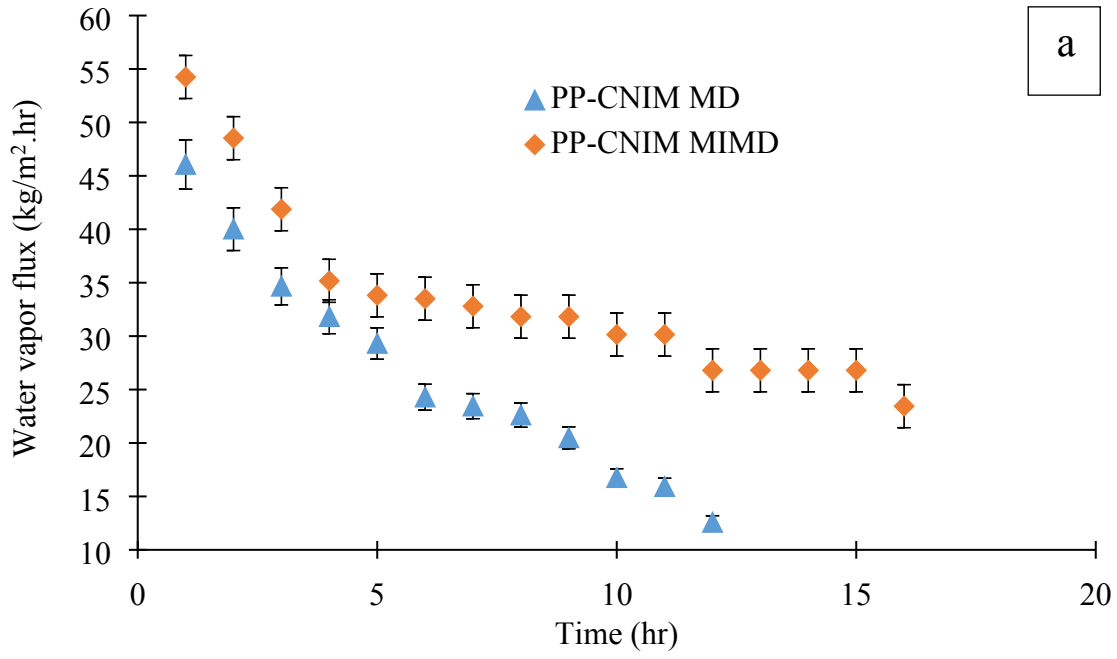

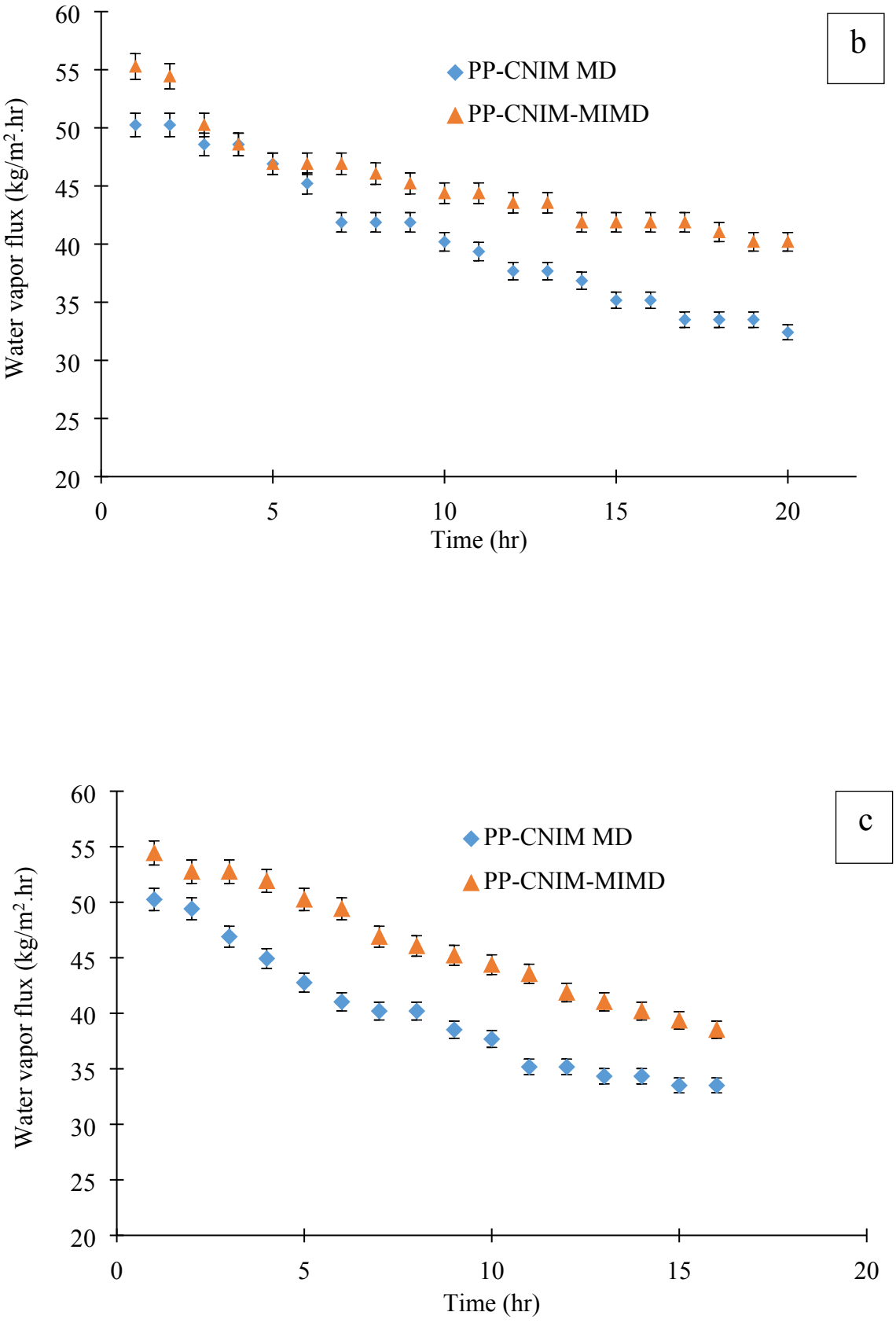

Figure 3. Water vapor flux in PP-CNIM membranes for **a)** $CaSO_4$ at a concentration of 2.95g/l, **b)** CaCO3 at a concentration of 3.5g/l , and **c)** $BaSO_4$ at a concentration of 2.5g/l. All analysis was done at a temperature of 70 °C and feed flow rate of 200 mL/min.

3.3. Deposition of salts on MD and MIMD membranes

The difference in the deposition of salt on CNIM by conventional MD and MIMD was quantified by weighing the amount of salt on the membrane before and after the experiment. The weight measurements were made after drying the membrane in an oven overnight at 70^{o}C. Special measures were taken to avoid any loss of deposited salt from the membrane surface during the removal of the membrane from the module and drying process. Table 1 shows that the total amount salt deposited on the membrane surface after 7 h of continuous operation at 70^{o}C under during MD and MIMD. The amount of salt deposited was significantly less, 50 to 79% for MIMD.

Table1. Deposition of salts on the membrane surface after 7 hrs of operation at 70^{o}C

Salt	**Amount of salt deposited on the membrane surface (mg)**		**% weight decrease**
	Conventional heating	**Microwave heating**	
$CaSO_4$	20.8	9.4	54.8
$CaCO_3$	7.1	1.5	78.9
$BaSO_4$	3.6	1.8	50.0

Membrane fouling was further investigated by characterizing the deposition of the respective salt crystals on the CNIM. **Figure 4a** and **4b** show SEM images of the original polypropylene membrane and the CNIM used in these experiments. The SEM images in Figure 4c to 4h were obtained from the membranes that were used to generate data described in Figure 3. **Figure 4c** and **4d** show the deposition of calcium sulfate crystal scales on CNIM after the experiments with conventional heating and microwave heating respectively. It is evident that the formation of calcium sulfate crystal on the membranes was significantly different in MD and MIMD. With conventional heating, calcium sulfate salt seemed to form homogeneous crystals that adhere to the membrane surface (**Figure 4c**), while such crystal formation was not observed in MIMD. Here the calcium sulfate crystals were small and non-

uniform, and the particles appeared to be sparsely dispersed certain areas on the membrane (**Figure 4d**). As a result, there was more active membrane surface available during MIMD that resulted in higher water vapor flux. Similar pattern of crystal formation was also observed in case of $CaCO_3$.With conventional MD, the rod like crystal of calcium carbonate densely packed the membrane surface (**Figure 4e),** whereas in MIMD, the crystals were smaller in size and flaky in nature with interstitial pores in-between them (**Figure 4f)**.

The deposition of barium sulfate on the membrane was also studied as illustrated in **Figure 4g** and **4h**. The crystals of barium sulfate salt with conventional heating appeared to be quite uniform and agglomerated (**Figure 4g**). While, with microwave heating, the particles were smaller and loosely deposited on the membrane surface (**Figure 4h**), so these resulted in higher flux enhancement for MIMD, compared to MD.

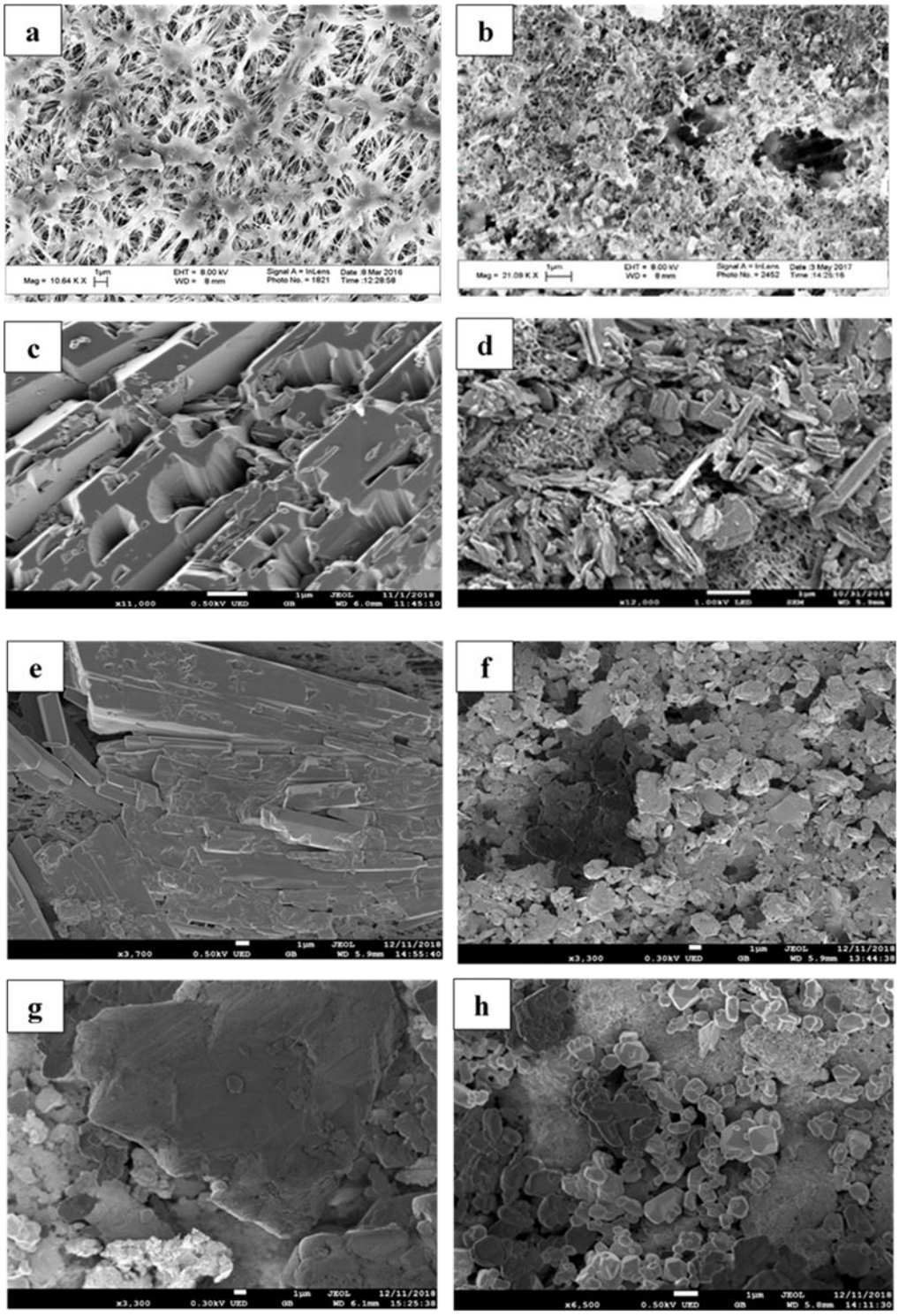

Figure 4. **a)** original PP membrane, **b)** CNIM, c) $CaSO_4$ scale with conventional heating, d) CaSO4 scale with MIMD, e**)** $CaCO_3$ scale with conventional heating, **f)** CaCO3 scale in MIMD, g) $BaSO_4$ scale with conventional heating, and **h)** BaSO4 scale with MIMD conventional heating, and **h)** BaSO4 scale with MIMD (The membranes in Figure 4c to 4h were obtained after completing the experiment described in Figure 3).

4. Proposed mechanism

Applying microwave heating of the brine during MD can affect the solution in different ways. The microwave heating breaks down the hydrogen bonded structure in the aqueous phase and disintegrate the salt particles present in the solution [44]**.** FTIR [44]and Raman [61] measurements have shown that the O-H band changes significantly in microwave treated water.

From nucleation theory [63], nucleation rate per volume is described by :

$$\mathbf{I} = \frac{\mathbf{D}}{R_d^2} n^{-\Delta G^*/KT}$$

where D is the diffusivity of nuclei, R_d is the space between the nuclei, ΔG* is the activation energy, K is the Boltzmann constant, and T is the temperature. D, R_d, as well as the activation energy can dramatically change the nucleus radius of salt under microwave radiations. Studies have also shown that the crystallization parameters including the nucleation coefficient, nucleation rate constant and the growth rate constant change significantly in microwave field [66, 67].

Another important consideration is the change in surface tension which is a measure of surface energy under microwave radiations. The reduction of surface tension is related to the nucleus radius salt granule by the equation below.

$$\boldsymbol{R}^* = \frac{-\mathbf{2\gamma}}{\Delta G_V}$$

Where R* is the critical nucleus radius, γ is the surface energy per area of nucleus or equal to σ (surface tension). Therefore, microwave radiation is expected to reduce surface tension, the nuclei radius and finally the size of the salt crystal. In addition, the nano-bubbles generated under microwave irradiation can also alter colloidal behavior of crystallizing salts, a phenomenon that has not been studied so far.

The influence of microwave heating on salt solutions was investigated by using FTIR spectroscopy and studying the alterations of the particle size via dynamic light scattering. The FTIR spectra of $CaSO_4$, $CaCO_3$ and $BaSO_4$ solution at room temperature (RT), conventional heating and microwave heating are presented in **Figure 5a**, **5b** and **5c**, respectively. As can be seen from the figures that the IR absorption of water molecules differed under conventional and microwave heating due to the variation in water-water and salt-water interactions [44]. The peak at 2127 cm^{-1} resulted from the combination of bending and liberations. The bending frequency at 1644 cm^{-1} was attributed to the hydrogen bonding, which was much weaker for microwave treated water for $CaSO_4$ solution. The peak at ~3490 cm^{-1} arose due to the stretching of water molecules. The nature of the spectrum was observed to be different under changing heating conditions as the arrangement of hydrogen bonded water clusters changed differently, which led to the variation of the peaks. The nature of FTIR spectra for $BaSO_4$ solution at 1644 cm^{-1} and ~3490 cm^{-1} were found to be slightly different than other Ca^{+2} salt solutions due to the difference in the ionic interactions of the corresponding salt solutions.

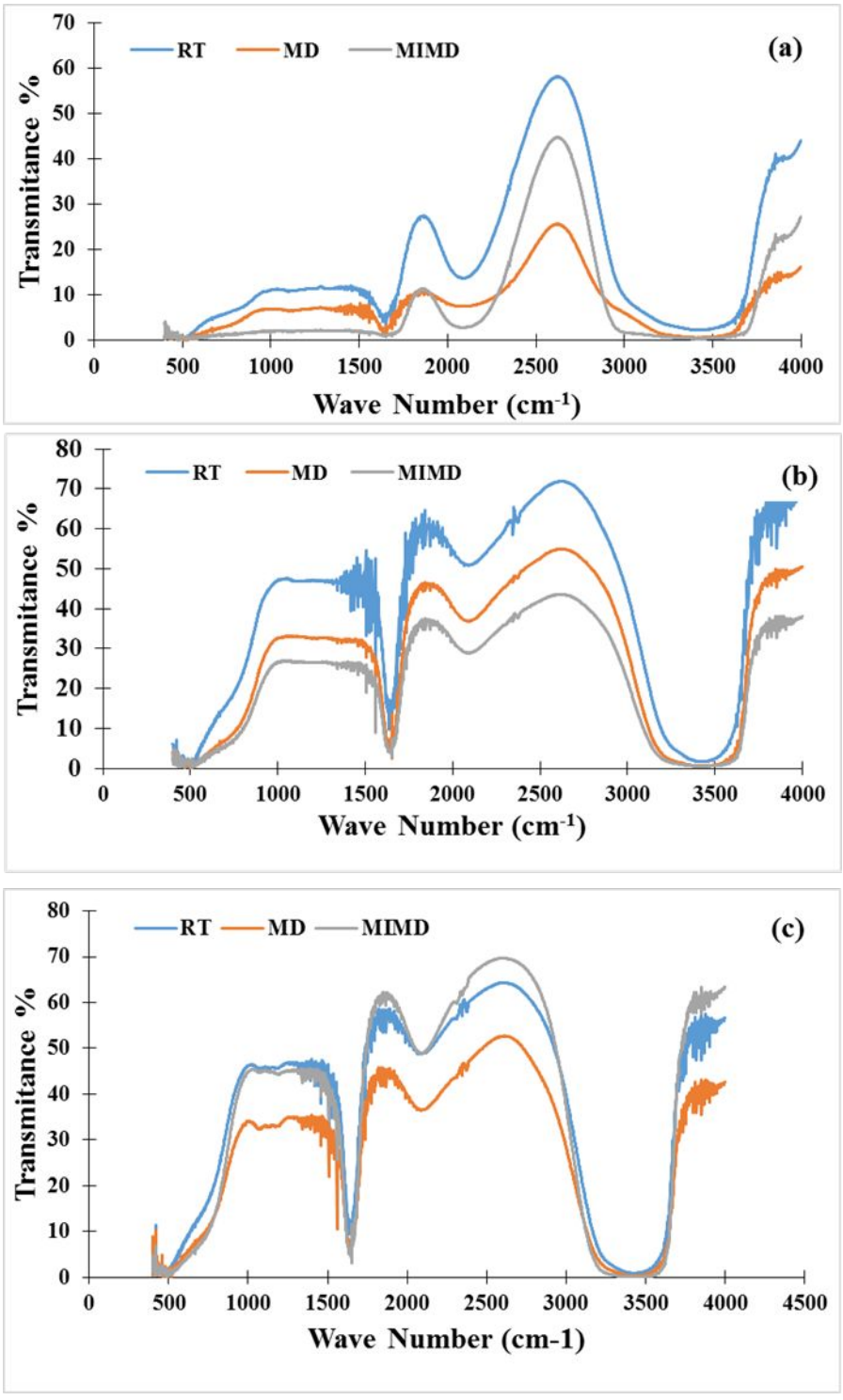

Figure 5. FTIR spectra of **a)** $CaSO_4$-water solution (2.95g/l); **b)** $CaCO_3$-water solution (3.5g/l); **c)** $BaSO_4$-water solution (2.5g/l) under room temperature (RT) microwave (MIMD) and conventional heating (MD).

Dynamic Light Scattering (DLS) was used to measure changes of the particle size of salt molecules after microwave irradiation compare to conventional heating. **Figure 6a** shows the influence of microwave irradiation on particle size distribution of $CaSO_4$. The average $CaSO_4$ particle size was 1173 nm at room temperature and dropped to 994 nm. at 70°C of regular heating, while it was 354 nm. when heated by the microwave heating at the same temperature. This showed that the microwave heating significantly lowered the average particle size of the $CaSO_4$ clusters. **Figure 6b** shows the influence of microwave heating on the particle size of $CaCO_3$ which was 1175 nm. at room temperature, and it dropped to 371 nm. at 70°C of regular heating and to 226 nm. during microwave heating. Similar influences were seen for $BaSO_4$ as shown in **Figure 6c**, where the particle size dropped from 827 nm. during regular heating to 362 nm. during microwave heating. In general, the particle size of all the salts above was significantly reduced by regular heating and microwave heating compared to what was observed at room temperature. This is in line with the previous report on crystallization in microwave activated water where microwave radiation led to a reduction in crystal lattice volume and crystal size compared to samples without microwave treatment [44].

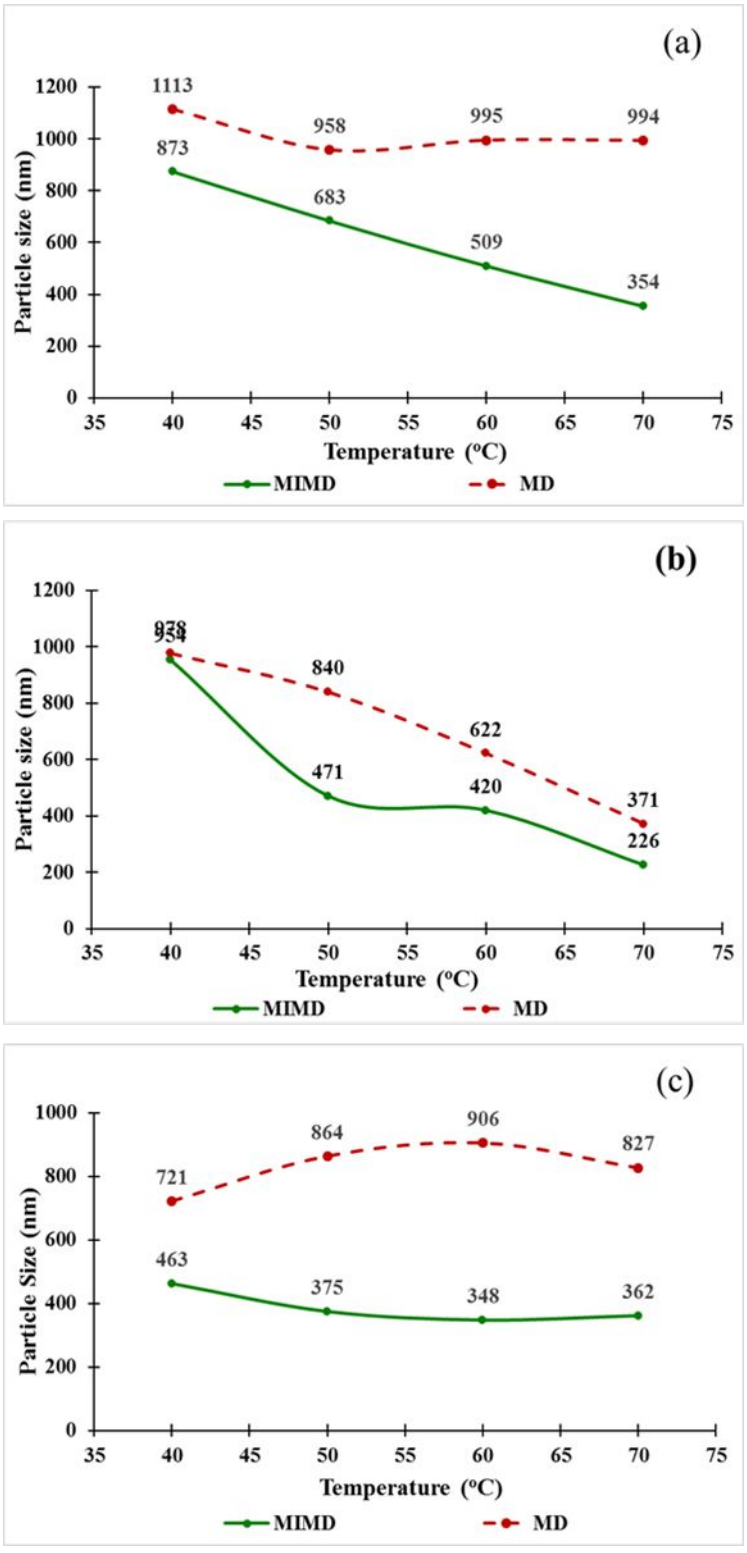

Figure 6. The influence of microwave irradiation on particle size distribution of **a)** $CaSO_4$; **b)** $CaCO_3$; and **c)** $BaSO_4$.

It is noted that the size reductions for $CaSO_4$, $CaCO_3$, and $BaSO_4$ were different. It appears that $BaSO_4$ was followed by $CaCO_3$, and $CaSO_4$. Among the other factors, the dissimilarities could be attributed to the difference in their dielectric constants. $BaSO_4$ had the highest dielectric constant, so it could absorb more energy and show more microwave effects while $CaCO_3$ had a higher electric constant than $CaSO_4$, which made the rate of size reduction of $CaCO_3$ higher than of $CaSO_4$.

5. Conclusions

In our previous study, we had demonstrated the performance enhancement of MIMD as compared to conventional MD. In this study, microwave irradiation was used as a means to heat the highly concentrated $CaCO_3$, $CaSO_4$ and $BaSO_4$ solutions in the DCMD mode. Besides the enhancement of water vapor flux, the MIMD exhibited significantly less fouling and the normalized flux decline was lower than conventional MD. The salt deposition on the membrane surface was observed to be between 50-79% less during MIMD and the morphology of the deposits from MIMD was quite different from those of conventional MD. It appears that non-thermal effect, such as, localized super heating, the breakdown of hydrogen bonding, alternation of surface tension, the increase in ionic mobility altered colloidal behavior and particle formation in MIMD. Apart from the less energy requirement and higher flux in MIMD, the lower flux decline at very high salt concentrations could lead to dramatic improvements to the MD technology in the future.

Acknowledgement:

This study was partially supported by a grant from the Chemical, Bioengineering, Environmental, and Transport Systems Division, National Science Foundation (grant number CBET-1603314).

References

1. Tong, T.; Elimelech, M., The global rise of zero liquid discharge for wastewater management: drivers, technologies, and future directions. *Environmental science & technology* **2016,** *50*, (13), 6846-6855.
2. Tsai, J.-H.; Macedonio, F.; Drioli, E.; Giorno, L.; Chou, C.-Y.; Hu, F.-C.; Li, C.-L.; Chuang, C.-J.; Tung, K.-L., Membrane-based zero liquid discharge: Myth or reality? *Journal of the Taiwan Institute of Chemical Engineers* **2017,** *80*, 192-202.
3. Nakoa, K.; Rahaoui, K.; Date, A.; Akbarzadeh, A., Sustainable zero liquid discharge desalination (SZLDD). *Solar Energy* **2016,** *135*, 337-347.
4. Chen, G.; Lu, Y.; Krantz, W. B.; Wang, R.; Fane, A. G., Optimization of operating conditions for a continuous membrane distillation crystallization process with zero salty water discharge. *Journal of Membrane Science* **2014,** *450*, 1-11.
5. Farahbod, F.; Mowla, D.; Nasr, M. J.; Soltanieh, M., Experimental study of forced circulation evaporator in zero discharge desalination process. *Desalination* **2012,** *285*, 352-358.
6. Al-Obaidani, S.; Curcio, E.; Macedonio, F.; Di Profio, G.; Al-Hinai, H.; Drioli, E., Potential of membrane distillation in seawater desalination: thermal efficiency, sensitivity study and cost estimation. *Journal of Membrane Science* **2008,** *323*, (1), 85-98.
7. Alkhudhiri, A.; Darwish, N.; Hilal, N., Membrane distillation: a comprehensive review. *Desalination* **2012,** *287*, 2-18.
8. Drioli, E.; Ali, A.; Macedonio, F., Membrane distillation: Recent developments and perspectives. *Desalination* **2015,** *356*, 56-84.
9. Wang, P.; Chung, T.-S., Recent advances in membrane distillation processes: Membrane development, configuration design and application exploring. *Journal of membrane science* **2015,** *474*, 39-56.
10. Souhaimi, M. K.; Matsuura, T., *Membrane distillation: principles and applications*. Elsevier: 2011.
11. Walton, J.; Lu, H.; Turner, C.; Solis, S.; Hein, H., Solar and waste heat desalination by membrane distillation. *Desalination and water purification research and development program report* **2004**, (81), 20.
12. Schwantes, R.; Cipollina, A.; Gross, F.; Koschikowski, J.; Pfeifle, D.; Rolletschek, M.; Subiela, V., Membrane distillation: Solar and waste heat driven demonstration plants for desalination. *Desalination* **2013,** *323*, 93-106.
13. Sarbatly, R.; Chiam, C.-K., Evaluation of geothermal energy in desalination by vacuum membrane distillation. *Applied Energy* **2013,** *112*, 737-746.
14. Gude, V. G., Exergy Evaluation of Desalination Processes. *ChemEngineering* **2018,** *2*, (2), 28.
15. Ali, E.; Orfi, J.; Najib, A.; Saleh, J., Enhancement of brackish water desalination using hybrid membrane distillation and reverse osmosis systems. *PloS one* **2018,** *13*, (10), e0205012.
16. Tan, Y. Z.; Wang, H.; Han, L.; Tanis-Kanbur, M. B.; Pranav, M. V.; Chew, J. W., Photothermal-enhanced and fouling-resistant membrane for solar-assisted membrane distillation. *Journal of Membrane Science* **2018,** *565*, 254-265.
17. Tan, Y. Z.; Ang, E. H.; Chew, J. W., Metallic spacers to enhance membrane distillation. *Journal of Membrane Science* **2019,** *572*, 171-183.

18. Tijing, L. D.; Woo, Y. C.; Choi, J.-S.; Lee, S.; Kim, S.-H.; Shon, H. K., Fouling and its control in membrane distillation—A review. *Journal of Membrane Science* **2015,** *475*, 215-244.
19. Gryta, M., Fouling in direct contact membrane distillation process. *Journal of membrane science* **2008,** *325*, (1), 383-394.
20. Warsinger, D. M.; Swaminathan, J.; Guillen-Burrieza, E.; Arafat, H. A.; Lienhard V, J. H., Scaling and fouling in membrane distillation for desalination applications: A review. *Desalination* **2015,** *356*, 294-313.
21. Biniaz, P.; Torabi Ardekani, N.; Makarem, M. A.; Rahimpour, M. R., Water and Wastewater Treatment Systems by Novel Integrated Membrane Distillation (MD). *ChemEngineering* **2019,** *3*, (1), 8.
22. Onsekizoglu, P., Membrane distillation: principle, advances, limitations and future prospects in food industry. In *Distillation-Advances from Modeling to Applications*, InTech: 2012.
23. Roy, S.; Bhadra, M.; Mitra, S., Enhanced desalination via functionalized carbon nanotube immobilized membrane in direct contact membrane distillation. *Separation and Purification Technology* **2014,** *136*, 58-65.
24. Bhadra, M.; Roy, S.; Mitra, S., Desalination across a graphene oxide membrane via direct contact membrane distillation. *Desalination* **2016,** *378*, 37-43.
25. Bhadra, M.; Roy, S.; Mitra, S., Enhanced desalination using carboxylated carbon nanotube immobilized membranes. *Separation and Purification Technology* **2013,** *120*, 373-377.
26. Bhadra, M.; Roy, S.; Mitra, S., Nanodiamond immobilized membranes for enhanced desalination via membrane distillation. *Desalination* **2014,** *341*, 115-119.
27. Bhadra, M.; Roy, S.; Mitra, S., Flux enhancement in direct contact membrane distillation by implementing carbon nanotube immobilized PTFE membrane. *Separation and Purification Technology* **2016,** *161*, 136-143.
28. Bhadra, M.; Roy, S.; Mitra, S., A bilayered structure comprised of functionalized carbon nanotubes for desalination by membrane distillation. *ACS applied materials & interfaces* **2016,** *8*, (30), 19507-19513.
29. Boo, C.; Lee, J.; Elimelech, M., Omniphobic polyvinylidene fluoride (PVDF) membrane for desalination of shale gas produced water by membrane distillation. *Environmental science & technology* **2016,** *50*, (22), 12275-12282.
30. Duong, H. C.; Chivas, A. R.; Nelemans, B.; Duke, M.; Gray, S.; Cath, T. Y.; Nghiem, L. D., Treatment of RO brine from CSG produced water by spiral-wound air gap membrane distillation—a pilot study. *Desalination* **2015,** *366*, 121-129.
31. Yu, X.; Yang, H.; Lei, H.; Shapiro, A., Experimental evaluation on concentrating cooling tower blowdown water by direct contact membrane distillation. *Desalination* **2013,** *323*, 134-141.
32. Roy, S.; Ragunath, S., Emerging Membrane Technologies for Water and Energy Sustainability: Future Prospects, Constraints and Challenges. *Energies* **2018,** *11*, (11), 2997.
33. Warsinger, D. M.; Tow, E. W.; Swaminathan, J., Theoretical framework for predicting inorganic fouling in membrane distillation and experimental validation with calcium sulfate. *Journal of Membrane Science* **2017,** *528*, 381-390.
34. Qasim, M.; Darwish, N.; Mhiyo, S.; Darwish, N.; Hilal, N., The use of ultrasound to mitigate membrane fouling in desalination and water treatment. *Desalination* **2018,** *443*, 143-164.
35. Ghadimkhani, A.; Zhang, W.; Marhaba, T., Ceramic membrane defouling (cleaning) by air Nano Bubbles. *Chemosphere* **2016,** *146*, 379-384.
36. Ye, Y.; Yu, S.; Hou, L. a.; Liu, B.; Xia, Q.; Liu, G.; Li, P., Microbubble aeration enhances performance of vacuum membrane distillation desalination by alleviating membrane scaling. *Water research* **2019,** *149*, 588-595.
37. He, F.; Sirkar, K. K.; Gilron, J., Effects of antiscalants to mitigate membrane scaling by direct contact membrane distillation. *Journal of Membrane Science* **2009,** *345*, (1-2), 53-58.
38. Greenlee, L. F.; Testa, F.; Lawler, D. F.; Freeman, B. D.; Moulin, P., The effect of antiscalant addition on calcium carbonate precipitation for a simplified synthetic brackish water reverse osmosis concentrate. *Water research* **2010,** *44*, (9), 2957-2969.
39. McCool, B. C.; Rahardianto, A.; Cohen, Y., Antiscalant removal in accelerated desupersaturation of RO concentrate via chemically-enhanced seeded precipitation (CESP). *Water research* **2012,** *46*, (13), 4261-4271.

40. Wang, J.; Sun, X.; Yuan, Y.; Chen, H.; Wang, H.; Hou, D., A novel microwave assisted photo-catalytic membrane distillation process for treating the organic wastewater containing inorganic ions. *Journal of Water Process Engineering* **2016,** *9*, 1-8.
41. Yatmaz, H. C.; Dizge, N.; Kurt, M. S., Combination of photocatalytic and membrane distillation hybrid processes for reactive dyes treatment. *Environmental technology* **2017,** *38*, (21), 2743-2751.
42. Qu, D.; Qiang, Z.; Xiao, S.; Liu, Q.; Lei, Y.; Zhou, T., Degradation of Reactive Black 5 in a submerged photocatalytic membrane distillation reactor with microwave electrodeless lamps as light source. *Separation and Purification Technology* **2014,** *122*, 54-59.
43. Ji, Z.; Wang, J.; Hou, D.; Yin, Z.; Luan, Z., Effect of microwave irradiation on vacuum membrane distillation. *Journal of membrane science* **2013,** *429*, 473-479.
44. Roy, S.; Humoud, M. S.; Intrchom, W.; Mitra, S., Microwave-Induced Desalination via Direct Contact Membrane Distillation. *ACS Sustainable Chemistry & Engineering* **2017,** *6*, (1), 626-632.
45. Galema, S. A., Microwave chemistry. *Chemical Society Reviews* **1997,** *26*, (3), 233-238.
46. Metaxas, A. a.; Meredith, R. J., *Industrial microwave heating*. IET: 1983.
47. Grant, E.; Halstead, B. J., Dielectric parameters relevant to microwave dielectric heating. *Chemical society reviews* **1998,** *27*, (3), 213-224.
48. Barba, A. A.; d'Amore, M., Relevance of dielectric properties in microwave assisted processes. In *Microwave materials characterization*, InTech: 2012.
49. D MP, M.; Baghurst, D., Applictions of mi-crowave dielectricheatingeffects to synthetic problems in chemistry. *Chem, Soc. Rev., voL2e, no 1*, 3-19.
50. Baffou, G.; Polleux, J.; Rigneault, H.; Monneret, S., Super-heating and micro-bubble generation around plasmonic nanoparticles under cw illumination. *The Journal of Physical Chemistry C* **2014,** *118*, (9), 4890-4898.
51. Wang, L.; Miao, X.; Pan, G., Microwave-induced interfacial nanobubbles. *Langmuir* **2016,** *32*, (43), 11147-11154.
52. Asakuma, Y.; Nakata, R.; Asada, M.; Kanazawa, Y.; Phan, C., Bubble formation and interface phenomena of aqueous solution under microwave irradiation. *International Journal of Heat and Mass Transfer* **2016,** *103*, 411-416.
53. Ji, Z.; Wang, J.; Yin, Z.; Hou, D.; Luan, Z., Effect of microwave irradiation on typical inorganic salts crystallization in membrane distillation process. *Journal of Membrane Science* **2014,** *455*, 24-30.
54. Cai, R.; Yang, H.; He, J.; Zhu, W., The effects of magnetic fields on water molecular hydrogen bonds. *Journal of Molecular Structure* **2009,** *938*, (1-3), 15-19.
55. Zhao, L.; Ma, K.; Yang, Z., Changes of water hydrogen bond network with different externalities. *International journal of molecular sciences* **2015,** *16*, (4), 8454-8489.
56. Sun, J.; Wang, W.; Yue, Q., Review on microwave-matter interaction fundamentals and efficient microwave-associated heating strategies. *Materials* **2016,** *9*, (4), 231.
57. Abramovitch, R. A., Applications of microwave energy in organic chemistry. A review. *Organic preparations and procedures international* **1991,** *23*, (6), 683-711.
58. Puligundla, P.; Abdullah, S.; Choi, W.; Jun, S.; Oh, S.; Ko, S., Potentials of microwave heating technology for select food processing applications: a brief overview and update. *Journal of Food Processing & Technology* **2013,** *4*, (11).
59. Fortuny, M.; Oliveira, C. B.; Melo, R. L.; Nele, M.; Coutinho, R. C.; Santos, A. F., Effect of salinity, temperature, water content, and pH on the microwave demulsification of crude oil emulsions. *Energy & Fuels* **2007,** *21*, (3), 1358-1364.
60. Parmar, H.; Asada, M.; Kanazawa, Y.; Asakuma, Y.; Phan, C. M.; Pareek, V.; Evans, G. M., Influence of microwaves on the water surface tension. *Langmuir* **2014,** *30*, (33), 9875-9879.
61. Rao, M. L.; Sedlmayr, S. R.; Roy, R.; Kanzius, J., Polarized microwave and RF radiation effects on the structure and stability of liquid water. *Current Science* **2010,** *98*, (11), 1500-1504.
62. Wojnarowicz, J.; Chudoba, T.; Gierlotka, S.; Lojkowski, W., Effect of Microwave Radiation Power on the Size of Aggregates of ZnO NPs Prepared Using Microwave Solvothermal Synthesis. *Nanomaterials* **2018,** *8*, (5), 343.
63. Yang, X.-q.; Yang, L.-j.; Huang, K.-m., Influence of Microwave Radiation on Growth of Calcium Sulphate Crystal by Monte Carlo Method. *Asian Journal of Chemistry* **2010,** *22*, (1), 781.

64. Pavlenko, V.; Lapteva, S.; Barbanyagre, V., Influence of Microwave Irradiation of Tempering Water on the Process of Crystallization of Calcium Sulfate Dihydrate. *Russian Physics Journal* **2017,** *60*, (7).
65. Gupta, O.; Roy, S.; Mitra, S., Enhanced membrane distillation of organic solvents from their aqueous mixtures using a carbon nanotube immobilized membrane. *Journal of Membrane Science* **2018,** *568*, 134-140.
66. Guo, Z.; Han, W.; Zhao, W.; Li, L.; Wang, B.; Xiao, Y.; Alopaeus, V., The effect of microwave on the crystallization process of magnesium carbonate from aqueous solutions. *Powder Technology* **2018,** *328*, 358-366.
67. Guo, Z.; Li, L.; Han, W.; Li, J.; Wang, B.; Xiao, Y., Interpretation of the microwave effect on induction time during CaSO4 primary nucleation by a cluster coagulation model. *Journal of Crystal Growth* **2017,** *475*, 220-231.